Available online at www.sciencedirect.com

ScienceDirect

Mendeleev Commun., 2021, **31**, 512–514

Mendeleev Communications

Structure and cytotoxicity of biodegradable poly(D,L-lactide-*co*-glycolide) nanoparticles loaded with oxaliplatin

Ekaterina V. Razuvaeva,*[a] Kirill T. Kalinin,[a] Nikita G. Sedush,[a] Alexey A. Nazarov,[b] Dmitry S. Volkov[b] and Sergei N. Chvalun[a,c]

[a] *National Research Center 'Kurchatov Institute', 123182 Moscow, Russian Federation. E-mail: razuvaeva.kate@gmail.com*
[b] *Department of Chemistry, M. V. Lomonosov Moscow State University, 119991 Moscow, Russian Federation*
[c] *N. S. Enikolopov Institute of Synthetic Polymeric Materials, Russian Academy of Sciences, 117393 Moscow, Russian Federation*

DOI: 10.1016/j.mencom.2021.07.025

Spherical nanoparticles based on the biocompatible and biodegradable poly(D,L-lactide-*co*-glycolide) copolymer (90 : 10) loaded with oxaliplatin were produced by nanoprecipitation. Effect of the oxaliplatin loading on structure, size and morphology of the copolymer particles is considered. The nanoformulation of oxaliplatin demonstrates enhanced cytotoxicity and selectivity *in vitro* against several cancer cells compared with the free drug.

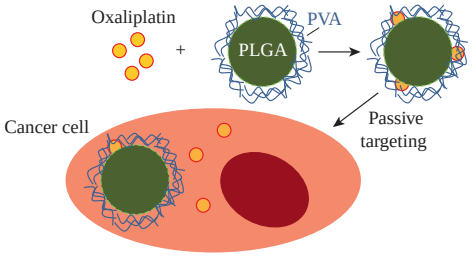

Keywords: lactide, glycolide, poly(lactide-*co*-glycolide), nanoparticles, oxaliplatin, drug delivery system.

Oxaliplatin or (*trans*-(*R*,*R*)-cyclohexane-1,2-diamine)oxalatoplatinum(II) is a third-generation Pt chemotherapy agent widely used for the treatment of colorectal cancer, with its clinical activity reported also for refractory or relapsed cases of ovarian, breast and germ cell cancers as well as lymphoma.[1] However, low water solubility of oxaliplatin, short half-life in the bloodstream and nonselective biodistribution hamper its therapeutic efficacy *in vivo*.[2] One of the ways to overcome the limits and improve the pharmacokinetics of this drug consists in a design of its nanoformulations. Nanocarriers such as liposomes,[3] polymeric particles,[4] dendrimers[5] and antibody-conjugated Au particles[6] have been proposed for targeted delivery of oxaliplatin. Poly(lactide) and its copolymers are among the most commonly used polymers in the design of biomedical materials, *e.g.*, surgical sutures, tissue engineering scaffolds and controlled drug delivery systems.[4,7–9] Polymeric particles based on poly(D,L-lactide-*co*-glycolide) (PLGA) are of interest as vehicles for drug delivery due to their biocompatibility and biodegradability.[10–14] Copolymerization of lactide with glycolide decreases hydrophobicity and enhances the polymer degradation rate, which allows one to control the release of incorporated pharmaceuticals. Solubilization of drug molecules using PLGA particles results in prolonged circulation time in the bloodstream, which is beneficial for passive targeting, and selective delivery to tissues including tumors due to so-called enhanced permeability and retention (EPR) effect,[15] improving the total therapeutic efficiency. Nevertheless, there are only a few works dedicated to PLGA particles as vehicles for anticancer Pt complexes.[16–18] In this work, we proposed a nanoformulation of oxaliplatin with PLGA nanoparticles and elucidated its structure and cytotoxicity.

PLGA copolymers used for production of nanoparticles typically contain 10–50 mol% glycolic acid residues. However, it is known that an increase in glycolide content from 10 to 25 mol% enhances the degradation of the polymer particles.[19,20] Here we used nanoparticles formed from a copolymer synthesized by the ring-opening copolymerization of D,L-lactide and glycolide in 90 : 10 ratio. Composition of the synthesized copolymer was confirmed by ^{1}H NMR (for details, see Online Supplementary Materials).

Aqueous suspensions of oxaliplatin-loaded and drug-free PLGA nanoparticles stabilized by poly(vinyl alcohol) (PVA) were produced by the known technique of nanoprecipitation.[21] Briefly, PLGA was dissolved in acetone, the solution was added dropwise to an aqueous solution of PVA with or without oxaliplatin, then the organic solvent was removed by evaporation. Drug loading content (DLC) for particles was determined by inductively coupled plasma atomic emission spectroscopy (ICP-AES) as 0.26 and 0.30 wt% with respect to the masses of PLGA and PVA, whereas the initial oxaliplatin content was 3 and 5 wt%, respectively, with the corresponding encapsulation efficiency of 8.7 and 6.0% (for details, see Online Supplementary Materials). The solubility of oxaliplatin in water is *ca.* 4–6 g dm^{-3}, so the hydrophilicity of the drug is supposed to hinder its encapsulation into hydrophobic PLGA core and leads to adsorption of its molecules at a core–corona interface of the particles. In this way, hydrophilization of the polymer *via* covalent bonding with poly(ethylene glycol) (PEG) facilitates the loading of oxaliplatin into the polymeric particles, as was found in our work for nanoparticles based on amphiphilic block copolymers PEG-*b*-poly(D,L-lactide) with higher values of the loading as well as encapsulation efficiency compared with their PLGA counterparts.[4]

Aqueous suspensions of the PLGA nanoparticles were explored using dynamic light scattering (DLS). Size distribution curves for all the samples reveal one peak (for details, see Online Supplementary Materials). The hydrodynamic radius values R_h corresponding to the peak DLS intensities of the size distribution curves are collected in Table 1 together with other physicochemical characteristics. Oxaliplatin loading does not affect the size of the nanoparticles in the limits of experimental uncertainty, similarly

Table 1 Physicochemical characteristics of the PLGA nanoparticles (see the text for parameters explanation).

Sample	Initial oxaliplatin content (wt%)	DLC (wt%)	R_h/nm	R_g/nm	$D_{max}/2$ /nm	R/nm	$2R_g/D_{max}$	R_g/R	ζ-potential/mV
1	0	0.00	77 ± 23	36.2 ± 0.1	54 ± 1	43 ± 1	0.67 ± 0.02	0.84 ± 0.03	–13 ± 1
2	3	0.26	76 ± 23	35.8 ± 0.1	53 ± 1	42 ± 1	0.68 ± 0.02	0.85 ± 0.03	–15 ± 1
3	5	0.30	69 ± 20	34.3 ± 0.1	51 ± 1	40 ± 1	0.67 ± 0.02	0.86 ± 0.03	–14 ± 1

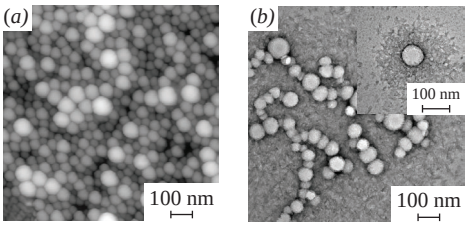

Figure 1 (*a*) AFM and (*b*) TEM images of the PLGA nanoparticles. Inset: the PLGA particle core surrounded by a PVA corona.

to the known data that the incorporation of vincristine and verapamil has no significant effect on the PLGA particles diameter.[10] The negative ζ-potential of the PLGA nanoparticles (see Table 1) can be explained by hydrolysis with formation of carboxylic groups on their surface.

Morphology of the PLGA nanoparticles was investigated by the atomic force microscopy (AFM) and transmission electron microscopy (TEM). All the particles have spherical shape (Figure 1) with an average diameter D evaluated from AFM and TEM being 52 ± 14 nm (for details, see Online Supplementary Materials). The value of D is considerably smaller than the corresponding values of hydrodynamic diameter $2R_h \approx 140$–155 nm (see Table 1), which can be explained by a higher contribution of stabilizing PVA corona to the R_h value.

Aqueous suspensions of the PLGA nanoparticles were investigated using the small-angle X-ray scattering (SAXS) (for details, see Online Supplementary Materials). The scattering curves for the particles in the coordinates log I *vs.* log s, where I is scattering intesity and s represents the momentum transfer, are presented in Figure 2(*a*). The SAXS profiles has secondary maxima at $0.1 < s < 0.3$ nm^{-1}, which allows one to suggest that the nanoparticles possess a well-defined spherical shape and a relatively narrow size distribution. The oxaliplatin loading does not affect notably the shape of the SAXS curves [see Figure 2(*a*)], *i.e.*, the structure and size of the PLGA nanoparticles remain unchanged with drug loading. However, an increase in the scattering intensity $I(s)$ of the loaded particles compared with the drug-free ones was observed on the SAXS profiles in the coordinates Is^2 *vs.* s [Figure 2(*b*)]. We suppose that this increment can be attributed to higher average electron density of the particles with encapsulated oxaliplatin compared with their drug-free counterparts.[4]

The plots of the pair distance distribution function $P(R)$ are presented in Figure 2(*c*). They are bell-shaped with a peak position value R of about a half of the maximum dimension of the scattering objects D_{max} (see Table 1), which is typical of homogeneous solid spherical particles.[22] From the gyraton radius R_g, the R_g/R ratios of 0.84–0.86 and $2R_g/D_{max}$ ratios of 0.67–0.68 (see Table 1) were derived, which allowed one to assume that structure of the PLGA nanoparticles was close to the spherical one with constant density ($R_g/R = 0.78$).

Antiproliferative activity of the oxaliplatin-loaded PLGA nanoparticles was investigated *in vitro* against human breast cancer MCF7 cells, human colon cancer HCT116 cells and human colon adenocarcinoma SW480 cells, for estimation of selectivity human lung carcinoma A549 cells and human non-cancer lung WI38 fibroblasts were also tested (for details, see Online Supplementary Materials). The activity was evaluated as a concentration of oxaliplatin that caused 50% inhibition of cell growth (IC_{50}), the resulting values are presented in Table 2. The loading of oxaliplatin in the particles results in its enhanced cytotoxicity compared with the free form. It has been reported[23] that PLGA nanoparticles with the size of 100–250 nm demonstrate high and fast uptake by HEK293 cells *via* endocytic pathway with a decrease in the size from 230 to 160 nm resulting in their enhanced endocytosis. Thus, the increase in IC_{50} values for the PLGA nanoparticles loaded with oxaliplatin could be attributed to their increased internalization into cancer cells compared with free oxaliplatin. Note that the *in vitro* cytotoxicity for cisplatin in its polymeric nanoformulations was reported as comparable with that of the free drug.[16,24]

The growth inhibitory activity of the drug-free PLGA nanoparticles and D-mannitol used as a cryoprotectant during the particles freeze-drying was estimated to be negligible for the cancer cell lines.

The selectivity of oxaliplatin loaded in the PLGA nanoparticles was investigated as comparison of the antiproliferative effects for carcinoma A549 cells and non-cancer WI38 fibroblasts. The selectivity coefficient k is 3.1–3.3, whereas that for free oxaliplatin equals *ca.* 0.5 (see Table 2), which is in accordance with known data[18] and suggests that the copolymer system proposed can decrease systemic toxicity. However, possible reasons for the selective action *in vitro* of the oxaliplatin-loaded PLGA nanoparticles are still unclarified and required further investigation.

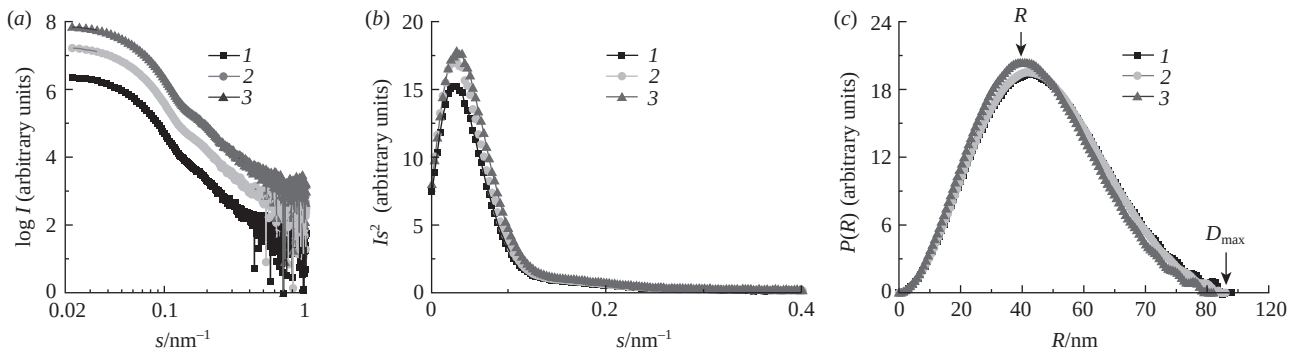

Figure 2 SAXS curves in the coordinates (*a*) log I *vs.* log s (the curves are shifted vertically for comparison), (*b*) Is^2 *vs.* s and (*c*) pair distance distribution functions $P(R)$ *vs.* R for (*1*) drug-free, (*2*) oxaliplatin-loaded particles with DLC of 0.26 wt% and (*3*) the particles with DLC of 0.30 wt% at 0.63 g dm^{-3} concentration.

Table 2 Antiproliferative effect of free oxaliplatin and PLGA nanoparticles loaded with oxaliplatin on the cancer cell lines MCF7, HCT116, SW480 and A549 as well as non-cancer cell line WI38.

Sample	IC_{50}/μM					k^a
	MCF7	HCT116	SW480	A549	WI38	
oxaliplatin	15.70 ± 1.30	12.97 ± 0.81	12.70 ± 1.14	29.30 ± 0.40	14.90 ± 1.59	0.5
PLGA + 0.26 wt% oxaliplatin	3.05 ± 0.53	1.19 ± 0.57	0.36 ± 0.31	2.98 ± 0.78	9.34 ± 0.93	3.1
PLGA + 0.30 wt% oxaliplatin	3.12 ± 0.16	3.90±0.70	3.80 ± 0.65	4.70 ± 0.46	15.41 ± 0.83	3.3

[a] Selectivity coefficient as a ratio of IC_{50} values for WI38 and A549 cells.

In summary, we have demonstrated that spherical PLGA nanoparticles represent a promising carrier for oxaliplatin. Loading of the PLGA particles with the drug does not affect their structure, size and morphology. Despite low values of DLC, namely 0.26 and 0.30 wt%, the nanoformulation of oxaliplatin reveals enhanced cytotoxicity to the cancer cell lines tested compared with the free drug, moreover, the selectivity of oxaliplatin increases *ca.* 6.4 fold after loading. We suggest that the nanoformulation of oxaliplatin based on the PLGA nanoparticles can enhance the efficiency of cancer therapy and decrease the adverse effects.

This work was supported by the Russian Science Foundation (grant no. 18-73-10079). The authors are grateful to The European Molecular Biology Laboratory (EMBL) for SAXS experiments employing the PETRA III storage ring of Deutsches Elektronen-Synchrotron, Hamburg. DLS, AFM and TEM measurements were carried out using equipment of the Resource Centers of the National Research Center 'Kurchatov Institute'. The authors are thankful to Dr. Dmitry R. Streltsov for the AFM experiments, Roman A. Kamyshinsky for the TEM experiments and Dr. Alevtina I. Kulebyakina for fruitful discussion.

Online Supplementary Materials

Supplementary data associated with this article can be found in the online version at doi: 10.1016/j.mencom.2021.07.025.

References

1 H. S. Oberoi, N. V. Nukolova, A. V. Kabanov and T. K. Bronich, *Adv. Drug Delivery Rev.*, 2013, **65**, 1667.
2 S. Dilruba and G. V. Kalayda, *Cancer Chemother. Pharmacol.*, 2016, **77**, 1103.
3 D. A. Arantseva and E. L. Vodovozova, *Russ. J. Bioorg. Chem.*, 2018, **44**, 619 (*Bioorg. Khim.*, 2018, **44**, 620).
4 Y. A. Kadina, E. V. Razuvaeva, D. R. Streltsov, N. G. Sedush, E. V. Shtykova, A. I. Kulebyakina, A. A. Puchkov, D. S. Volkov, A. A. Nazarov and S. N. Chvalun, *Molecules*, 2021, **26**, 602.
5 A. Narmani, M. Kamali, B. Amini, A. Salimi and Y. Panahi, *Process Biochem.*, 2018, **69**, 178.
6 S. Tummala, M. N. S. Kumar and S. K. Pindiprolu, *Drug Delivery*, 2016, **23**, 3505.
7 H. Cabral, K. Miyata, K. Osada and K. Kataoka, *Chem. Rev.*, 2018, **118**, 6844.
8 E. V. Razuvaeva, A. I. Kulebyakina, D. R. Streltsov, A. V. Bakirov, R. A. Kamyshinsky, N. M. Kuznetsov, S. N. Chvalun and E. V. Shtykova, *Langmuir*, 2018, **34**, 15470.
9 E. S. Trofimchuk, M. A. Moskvina, O. A. Ivanova, V. V. Potseleev, V. A. Demina, N. I. Nikonorova, A. V. Bakirov, N. G. Sedush and S. N. Chvalun, *Mendeleev Commun.*, 2020, **30**, 171.
10 X. Song, Y. Zhao, W. Wu, Y. Bi, Z. Cai, Q. Chen, Y. Li and S. Hou, *Int. J. Pharm.*, 2008, **350**, 320.
11 K. S. Yadav and K. K. Sawant, *AAPS PharmSciTech.*, 2010, **11**, 1456.
12 V. Yu. Balabanyan, A. M. Ul'yanov, V. Bojat, A. Yu. Khomenko, N. G. Sedush, S. N. Chvalun, G. D. Kapanadze, Y. M. Hamdy and V. I. Shvets, *Biofarm. Zh.*, 2013, **5** (6), 28 (in Russian).
13 S. Pieper and K. Langer, *Mater. Today: Proc.*, 2017, **4**, S188.
14 F. Madani, S. S. Esnaashari, B. Mujokoro, F. Dorkoosh, M. Khosravani and M. Adabi, *Adv. Pharm. Bull.*, 2018, **8**, 77.
15 H. Maeda, *J. Controlled Release*, 2012, **164**, 138.
16 E. C. Gryparis, M. Hatziapostolou, E. Papadimitriou and K. Avgoustakis, *Eur. J. Pharm. Biopharm.*, 2007, **67**, 1.
17 A. C. Jayasuriya and A. J. Darr, *J. Biomed. Sci. Eng.*, 2013, **6**, 586.
18 A. L. C. de S. L. Oliveira, R. F. de Araújo, Jr., T. G. de Carvalho, A. B. Chan, T. Schomann, F. Tamburini, L.-F. de Geus-Oei and L. J. Cruz, *Pharmaceutics*, 2020, **12**, 193.
19 T. G. Park, *Biomaterials*, 1995, **16**, 1123.
20 Yu. V. Ermolenko, A. S. Semyonkin, Yu. V. Ulianova, T. S. Kovshova, O. O. Maksimenko and S. E. Gelperina, *Russ. Chem. Bull., Int. Ed.*, 2020, **69**, 1416 (*Izv. Akad. Nauk, Ser. Khim.*, 2020, 1416).
21 H. Fessi, F. Puisieux, J. P. Devissaguet, N. Ammoury and S. Benita, *Int. J. Pharm.*, 1989, **55**, R1.
22 D. I. Svergun and M. H. J. Koch, *Rep. Prog. Phys.*, 2003, **66**, 1735.
23 A. Sahin, G. Esendagli, F. Yerlikaya, S. Caban-Toktas, D. Yoyen-Ermis, U. Horzum, Y. Aktas, M. Khan, P. Couvreur and Y. Capan, *Artif. Cells, Nanomed., Biotechnol.*, 2017, **45**, 1657.
24 X. Li, R. Li, X. Qian, Y. Ding, Y. Tu, R. Guo, Y. Hu, X. Jiang, W. Guo and B. Liu, *Eur. J. Pharm. Biopharm.*, 2008, **70**, 726.

Received: 25th February 2021; Com. 21/6465